Journal of Power Sources 203 (2012) 184–189

Contents lists available at SciVerse ScienceDirect

Journal of Power Sources

journal homepage: www.elsevier.com/locate/jpowsour

A battery with variable electrostatic capacity controlled by redox reaction

Jiro Sakata*

Advanced Battery Lab., Electrochemistry Div., Toyota Central R&D Labs., Inc., Yokomichi, Nagakute, Aichi 480-1192, Japan

ARTICLE INFO

Article history:
Received 13 September 2011
Received in revised form 1 November 2011
Accepted 6 December 2011
Available online 18 December 2011

Keywords:
Rechargeable battery
Capacitor
Variable electrostatic capacity
Sulfur composite material
Anthracene

ABSTRACT

A battery with variable electrostatic capacity is proposed as a new type battery with increased capacity. If the electrostatic capacity can be significantly changed by redox, then the capacity of a capacitor can be superimposed on the capacity of the battery. Calcination of a mixture of anthracene and sulfur was performed to prepare a sulfur composite material (ANS450) as a model material. Elemental analysis and Raman spectroscopy indicated that ANS450 has a structure in which anthracene frames combined with sulfur are linked together by dithiane structures. Although XPS analysis indicated that sulfur in ANS450 performed a one-electron reduction, ANS450 exhibited an extremely large capacity of 0.86 Ah g^{-1}, which was larger than the capacity estimated from the sulfur content. Cyclic voltammetry revealed that the electrostatic capacity of ANS450 was significantly changed by redox. This change in electrostatic capacity is considered to be the main factor for the increase in capacity, which validates the basic concept of a battery with variable electrostatic capacity.

1. Introduction

In recent years, demand has increased for batteries with ultrahigh energy densities exceeding 1000 Wh L^{-1} for portable electronics and electrical applications such as cellular phones and notebook computers, in addition to electric and hybrid vehicles. Many trials have employed simple substances as active materials for high-capacity batteries, such as Li-sulfur and Li-air batteries [1–3]. In the Li-sulfur battery, polysulfide ions are dissolved in the electrolyte solution and the shuttle phenomenon occurs, causing problems such as self-discharge, which in turn lowers the charge–discharge efficiency [4–7]. Sulfur fixation and the use of composites with carbon have been proposed to solve these problems [8–15]. In the case of sulfur fixation, sulfur bonded to carbon undergoes a one-electron reduction, and because the polymer structure used to fix sulfur does not act as an active material, the capacity falls to a value below half that of elemental sulfur. Prevention of sulfur dissolution can be achieved by distribution of sulfur in carbon; however, the capacity of this configuration is not sufficient. Thus, an ultrahigh energy density battery has yet to be realized.

To realize a battery with high energy density is difficult using only conventional electrochemical principles, such as the redox phenomenon. Therefore, a new approach, such as the fusion of chemical and physical phenomena, is required. For example, ruthenium acid nanosheets and mesoporous TiO_2 have been known as the pseudocapacitors which show Faradaic and non-Faradaic phenomena [16–18]. In this paper, an idea, which I have named a "battery with variable electrostatic capacity", is proposed to increase the capacity of an energy storage device.

If the electrostatic capacity of a capacitor can be changed by application of a certain voltage, then a large electric charge is generated and the capacitor exhibits an output similar to a battery, which charges and discharges at constant potential. If redox becomes a trigger and the electrostatic capacity can be changed, then an output characteristic can be realized where the capacity of the capacitor is superimposed on the redox capacity. Even if the applied voltage is limited to a narrow range in which redox occurs, a large capacitor capacity that is proportional to the difference between the spontaneous potential and the redox potential can be generated.

I consider that a compound possessing electroconductive structures, such as polycyclic aromatic structures with redox groups such as disulfide groups, is capable of significant change in the electrostatic capacity at the redox potential. In this paper, a composite material of sulfur combined with anthracene was prepared as the material, and validation of the "battery with variable electrostatic capacity" idea was attempted.

2. Experimental

2.1. Materials

Anthracene (Aldrich, 1 g, 5.6 mmol) and excess amounts of sulfur powder (Kojundo Chemical Laboratory, 5 g, 20 mmol of S_8) were mixed and placed into a test tube. The test tube was set in a tubular furnace under nitrogen flow and the temperature was raised to

* Tel.: +81 561717683; fax: +81 561635743.
E-mail address: sakata@mosk.tytlabs.co.jp

0378-7753/$ – see front matter © 2012 Published by Elsevier B.V.
doi:10.1016/j.jpowsour.2011.12.006

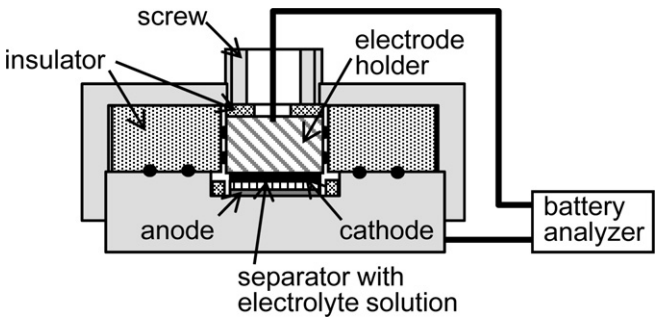

Fig. 1. Schematic diagram of the pressurized coin type cell.

300 °C over 1 h. After holding at 300 °C for 3 h, the temperature was raised to 450 °C over 30 min and then held at 450 °C for 3 h in order to remove excess sulfur. The resulting black product (ANS450) was obtained after cooling to room temperature.

2.2. Electrochemical evaluation

ANS450 (70 wt%) or elemental sulfur S_8 (50 wt%) was mixed with polytetrafluoroethylene (PTFE; 10 wt%) and carbon (Ketjen black; residual amounts) using ethanol as a dispersant. The mixture was ground using a mortar and a pestle to form a paste. The ground electrode material was formed into a sheet from which a 12 mm diameter electrode (typical weight: 3.0 mg) was then cut. The vacuum dried electrode was used as a cathode. A schematic diagram of the pressurized coin type cell employed is shown in Fig. 1. A 1 M $LiPF_6$ solution in ethylene carbonate/diethyl carbonate (EC/DEC, volume ratio: 3/7) was used as an electrolyte for the Li-ANS450 cell. In the case of the Li-S_8 cell, carbonate solvents such as EC and DEC cannot be used because sulfide ion reacts with these solvents. Therefore, a 1 M lithium bis(trifluoromethansulfonyl)imide solution in dimethoxyethane/dioxolane (DME/DOL, volume ratio: 9/1) was used as an electrolyte for the Li-S_8 cell. A porous polyethylene membrane and Li foil were used as the separator and anode, respectively. The anode, separator, and cathode were placed in the cell from the bottom with the electrolyte solution and the electrodes were pressurized using the upper screw to make an electrical contact. The coin cell was assembled in an Ar-filled glove box. Galvanostatic charge–discharge measurements were performed at 25 °C using a battery analyzer (HJ-1001, Hokuto Denko). For initial aging of the cell, charge–discharge cycles were carried out twice between 0.3 and 3 V at a constant current of 0.5 mA. The charge–discharge characteristics were measured in the range of 1–3 V at a constant current of 0.5 mA.

Cyclic voltammetry (CV) was measured with an electrochemical interface (Solartron SI 1287) using the same cell as that used for the charge–discharge characteristics. The sweep rates were 0.86, 1.4, 3.6, and 7.1 mV s^{-1} and the scanning voltage ranges were 1–3, 1–2, and 2.2–3 V.

2.3. Characterization

ANS450 was characterized using elemental analysis, Raman spectroscopy, X-ray photoelectron spectroscopy (XPS; Ulvac Phi, model HI-5500MC), and X-ray diffraction (XRD; Rigaku, RINT-TTR, Cu Kα radiation) analysis. The Raman spectrum was recorded with a Jasco NRS-3300 Laser Raman Spectrophotometer, using the 532 nm line of a Nd:YVO4 laser as an excitation source. As a model compound for Raman analysis, hexathiapentacene (HTP) was prepared by the method reported in the literature [19]. Simulation of the Raman spectrum was performed by *ab initio* HF/3-21G calculations with Gaussian 03 [20]. XPS and XRD analyses were conducted for samples of the cathode (ANS450:90 wt%, PVDF or PTFE and carbon: 5 wt%) before and after charge–discharge without exposure to air. The cathodes for the XPS analysis were ground well to form powder using a mortar and a pestle in the Ar-filled glove box. As an authentic sample of the S_{2p} XPS spectrum, Li_2S_x deposited on Li anode in S_8 cell after cycle tests was employed.

3. Results and discussion

3.1. Structure of ANS450

Elemental analysis of ANS450 revealed an elemental ratio of C:H:S:(O) = 14:0:7.8:(0.6). Although a small amount of oxygen was included, the elemental ratio was mostly in agreement with a C:S = 14:8 structure, as shown by structural formula 1, in which hydrogen in anthracene is replaced by sulfur and the anthracene rings are linked together by dithiane structures (Scheme 1).

Fig. 2 shows the Raman spectra of ANS450 and the model compound HTP, and a simulated spectrum based on structural formula 1. The peaks in the range of 100–1100 cm^{-1} can be attributed mostly to the structure containing sulfur, C—S and S—S [21,22], and the peaks in the range of 1100–1600 cm^{-1} are due to the aromatic series ring frame [23]. The peaks around 100–1100 cm^{-1} of HTP possessing six sulfur atoms connected with aromatic rings are coincident with those of ANS450. Other peaks observed in the range of 100–1100 cm^{-1} (a)–(d) were assigned to γCS, νCS, δCSC, and δCSC, respectively, according to the literature examining Raman spectroscopy of thiathrene possessing the dithian structure [21]. The strong peak (a) was also assigned to C=S stretching [22]. The peaks in the range of 1100–1600 cm^{-1} are in good agreement with the simulated spectrum. Therefore, both Raman spectroscopy and elemental analysis indicate that the main component of ANS450 has the structure of formula 1. In addition, no peaks characteristic of elemental sulfur (indicated with three triangle marks) are evident in Fig. 2, which indicates the absence of sulfur in the form of isolated S_8.

Fig. 3 shows the S_{2p} XPS spectra of the cathodes before and after charge–discharge, and that of Li_2S_x. The XPS S_{2p} spectrum of Li_2S_x has three peaks. According to the literature which examined Li-polysulfide deposited on Li metal [24], the S_{2p} peaks of S bridging S, Li_2S_2, and Li_2S appear at 164 eV, 161.5 eV, and 160.0 eV, respectively. It was reported that the S_{2p} peak of hexathiaanthracene was

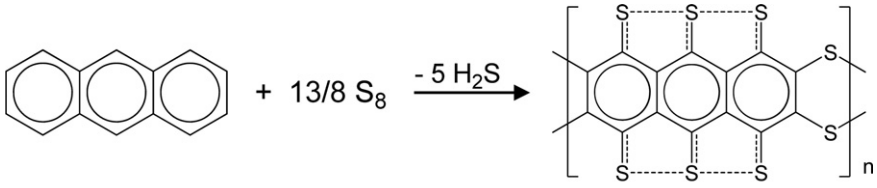

Structural formula 1

Scheme 1. Synthetic reaction and structural formula 1.

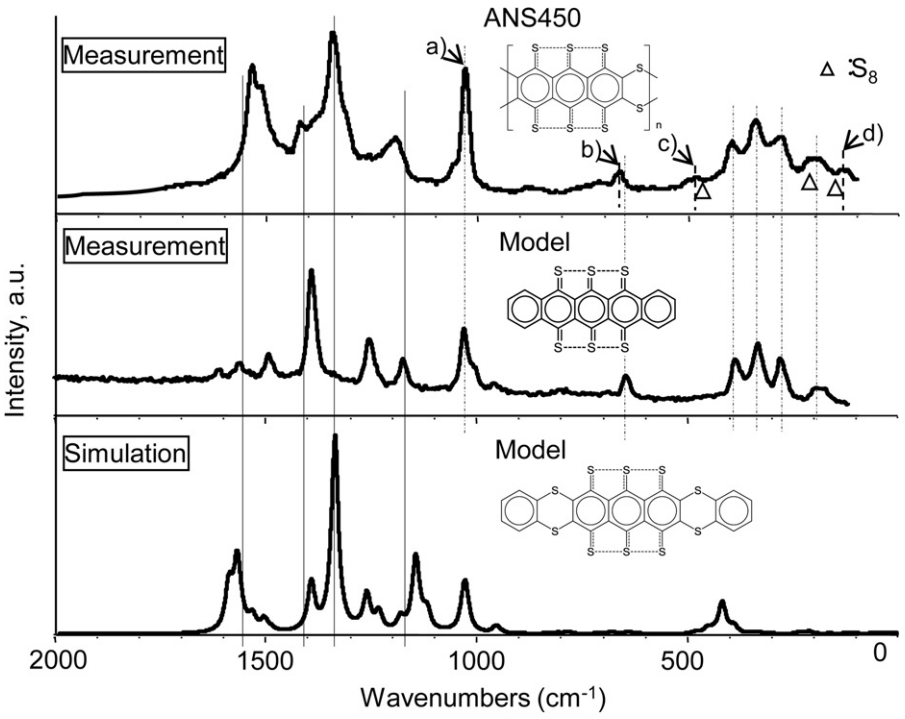

Fig. 2. Raman spectra of ANS450 and the model compound hexathiapentacene, and a simulated spectrum of a model compound. (Triangle marks indicate the characteristic peaks of elemental sulfur S_8. (a)–(d) indicate the characteristic peaks of thiathrene possessing the dithian structure.)

located at 163.5 eV [25]. Therefore, three peaks observed in the Li_2S_x sample are attributed to neutral sulfur, univalent sulfide anion, and divalent sulfide anion in order of higher bonding energy. The intact ANS450 sample showed almost one peak at 163.1 eV, which is identified as neutral sulfur in the structure of C—S—S—C or C—S—C. The S_{2p} peak of the discharged sample was shifted to 161.4 eV, which is identified as the univalent sulfide anion, and that of the charged sample was returned to 163.1 eV. This change occurs reversibly. The results indicate that sulfide undergoes reversible redox during the charge–discharge process. The peak at 160.0 eV, which represents the divalent sulfide anion, Li_2S, was not observed.

The XRD patterns of the intact cathode (before charge–discharge) and that after discharge or charge are shown in Fig. 4. The XRD pattern of the discharged sample exposed to air is also shown in Fig. 4. A relatively strong peak at 3.54 Å is observed for the intact cathode, in addition to several weak peaks. According to the literature of HTP, the spacing of π–π stacking of pentacene rings is 3.54 Å [19]. Therefore, ANS450 appears to have the π–π stacking structure. The XRD pattern of the discharged cathode shows that the peaks observed for the intact cathode disappeared, and a new broad peak appeared at 3.3 Å, which indicates that the stacking structure is collapsed by aging and/or discharge, and discharged ANS450 has a slightly regulated structure by weak interaction between molecules. After charging, the 3.3 Å

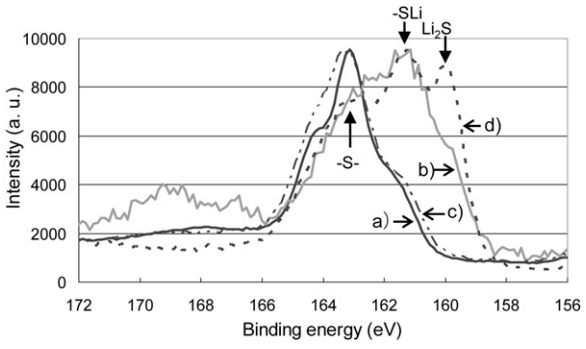

Fig. 3. XPS S_{2p} spectra of sulfur in ANS450 (a) before discharge/charge, (b) after 1st discharge, (c) after 1st charge, and (d) Li_2S_x.

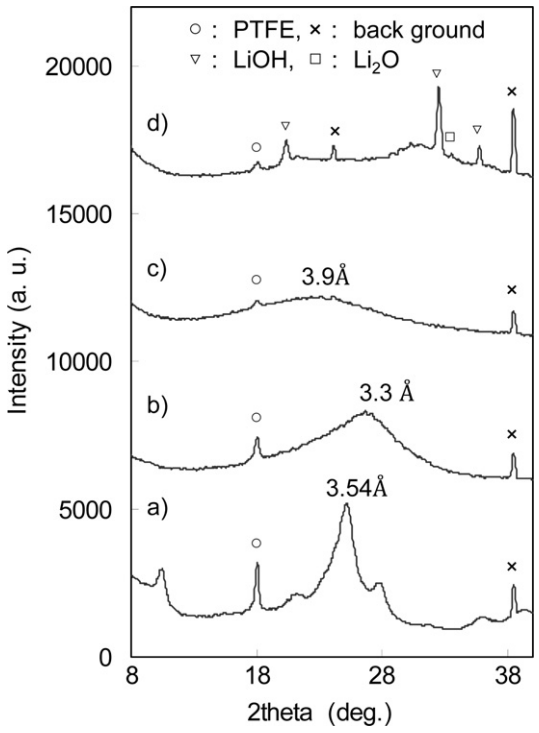

Fig. 4. XRD patterns of ANS450 cathodes (a) before discharge/charge, after (b) discharge, and (c) charge, and (d) after discharge with exposure to air for 1 h (the background peaks were observed from the XRD vessel without a sample).

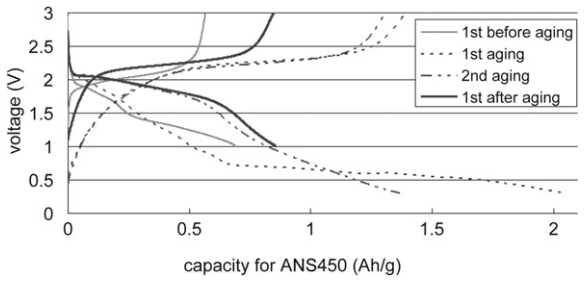

Fig. 5. Charge and discharge curves before, during, and after aging.

peak disappeared and a broad halo peak appeared near 3.9 Å. This change occurs reversibly (not shown in Fig. 4). The charged cathode has an amorphous structure, although the oxidation state of sulfide in charged ANS450 remains the same as that in intact ANS450, as shown in Fig. 3. It seems that intermolecular disulfide bonds are formed in addition to intramolecular bonds by oxidation, and the structure of charged ANS450 becomes crosslinked and amorphous. Several peaks, which were identified as LiOH or Li_2O, were observed in the XRD pattern of the discharged sample after exposure to air for 1 h. This result indicates that Li ions are eliminated from the composite material by oxidation.

As described in Section 2, heat treatment of ANS450 was performed under N_2 flow for 3 h at 450 °C higher than the boiling point of elemental sulfur, therefore it was expected that sulfur without fixation to carbon was removed in the form of elemental sulfur. When EC/DEC is used as the solvent of electrolyte for the Li-sulfur cell, first discharged capacity decreases to a half value of the capacity of Li-sulfur cell using DME/DOL as the solvent. Furthermore charge and discharge cannot be done after the first discharge. The Li-ANS450 cell showed excellent repeatability of charge–discharge, although the solvent of electrolyte was EC/DEC. This result indicates that active material in the Li-ANS450 is different from that in the Li-sulfur cell, elemental sulfur.

XPS analysis, Raman spectroscopy, and examination of the solvent effect indicate that sulfur in ANS450 combined with carbon and performs a one-electron reduction during the discharge process.

3.2. Charge–discharge characteristics

Fig. 5 shows the charge–discharge characteristics for the first cycle before aging, during aging, and the first cycle after aging. The discharge voltage before aging was slightly low and the voltage rose after aging. As mentioned in the XRD results, the stacking structure of ANS450 is collapsed by aging and/or discharge. The aging acts as an electric activation of carbon usually operated for capacitor materials. Large irreversible capacity was observed at the first aging. When a cathode without ANS450 consisting of only Ketjen black and PTFE was aged until 0.3 V, huge irreversible capacity was observed. When concentration of ANS450 was increased to 90%, the irreversible capacity during aging decreased to 1/3. Therefore, it seems that the irreversible capacity of the Li-ANS450 cell during aging mainly arose from Ketjen black and/or PTFE binder. The discharge capacity of the first cycle after aging was extremely large at 0.86 Ah g^{-1}-ANS450, and 1.47 Ah g^{-1}-sulfur content. When all the sulfur bonded to carbon is assumed to undergo a one-electron reduction, the capacity was estimated at 0.49 Ah g^{-1}. The capacity of ANS450 exceeds the capacity estimated from the sulfur content. XPS analysis indicated the absence of Li_2S in discharged ANS450; therefore, it can be concluded that the large capacity of ANS450 is not due to a mixture with isolated S_8, which undergoes two-electron reduction.

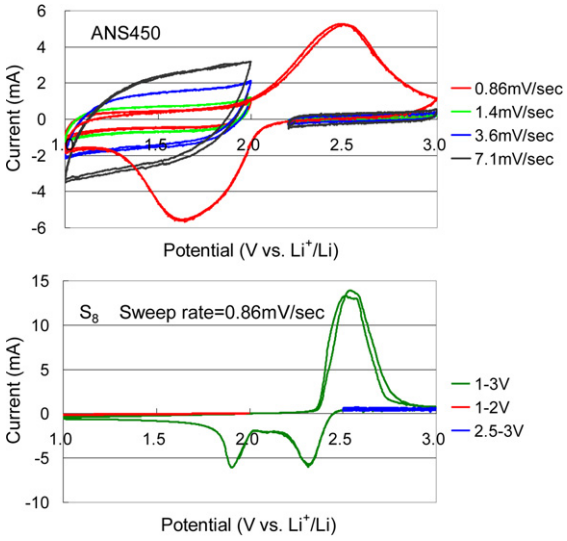

Fig. 6. Cyclic voltammograms for cells with ANS450 and sulfur (S_8) cathodes.

3.3. Variable electrostatic capacity

In order to clarify the mechanism for generation of capacity greater than the estimated value from sulfur content, CV of ANS450 and elemental sulfur (S_8) was measured in three ranges of scanning voltage; 1–3 V extensive voltage range, 1–2 V low-voltage range, and 2.2–3 V high-voltage range, and the results are shown in Fig. 6. When S_8 was used as the active material, one oxidation (charge) peak and two reduction (discharge) peaks were observed in the 1–3 V range, and both the high-voltage range scans after charge and the low-voltage range scan after discharge showed narrow width CV characteristics without peaks. A narrow width CV waveform indicates only a small electrostatic capacity when S_8 is used as the active material. In contrast, oxidation and reduction peaks for ANS450 were observed in the 1–3 V range scan, while no peaks were observed in either the high-voltage or low-voltage range scans. However, the low-voltage range scan showed a broad rectangular waveform that became thin in the high-voltage range scan. The rectangular waveform was symmetrical and became broader with increasing scan rate. The width of the rectangular waveform is proportional to the electrostatic capacity of the capacitor composition; therefore, ANS450 exhibits variable electrostatic capacity in which the electrostatic capacity is decreased by charge (oxidation) and increased by discharge (reduction). The electrostatic capacity for ANS450 was 45 F g^{-1} in the high-voltage range and was increased to 290 F g^{-1} in the low-voltage range, which is an increase of 6.5 times. Compared with the electrostatic capacity of activated carbon used for an electric double layer type capacitor of approximately 100 F g^{-1} [26], the electrostatic capacity of ANS450 in the low-voltage range is extremely large. The proportionality constant of capacitance is 5–7 μF cm^{-2} for an electric double layer type capacitor; therefore, the effective electrode area of ANS450 can be calculated as 4000–6000 m^2 g^{-1}, which is too large compared with the surface area of graphene (2620 m^2 g^{-1}). ANS450 has a linear structure and the effective electrode area of the rod-like ANS450 molecule may become much larger than that of the flat-shaped graphene molecule.

Supposing that discharge was conducted under a voltage difference of 2.25 V between the onset voltage of 3.25 V and the minimum applied voltage of 1 V, the capacity of the capacitor composition calculated from the electrostatic capacity of the low-voltage range would be 0.18 Ah g^{-1}. The entire discharge capacity measured just before CV measurement and the capacity calculated from the sulfur

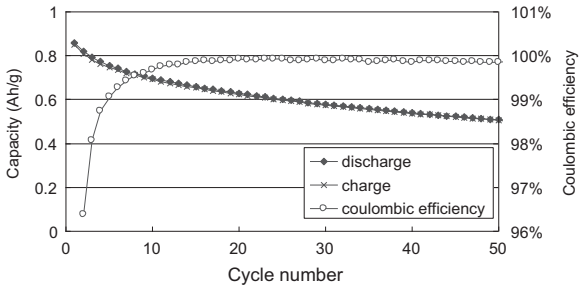

Fig. 7. Charge–discharge cycling characteristics of the cell with the ANS450 cathode.

content were 0.73 and 0.49 Ah g^{-1}, respectively. Thus, the increase in capacity from the estimated capacity to the entire discharge capacity was 0.24 Ah g^{-1}. Although the capacity of the capacitor is slightly smaller than the increase in capacity, it provides the main contribution to the increase in capacity.

3.4. Mechanism of variable electrostatic capacity

From the CV and XRD measurement results, I propose the following electrostatic capacity change mechanism. The polycyclic aromatic rings in intact ANS450 were stacked in layers, so that ions could not penetrate between the layers above 1 V, but only the bulk surface acted as the area of the electric double layer capacitor. If the aging voltage until 0.3 V was applied, then the aromatic rings separated, probably due to penetration of Li ions, and the stacking structures collapsed; this is similar phenomenon to the activation process for carbon electrode used in capacitors. Cations could penetrate and adsorb on the aromatic rings in the form of electric double layers; therefore, each molecular chain acted as the rod-like electrode of a capacitor. As a result, the effective area was significantly increased, and an increase in the electrostatic capacity was able to be realized.

During the charging process, sulfide anions were oxidized to form disulfide bonds, however, higher-order steric information could not be obtained from the XRD results. Since ANS450 became amorphous after charging, I assume that intermolecular disulfide bonds were formed in addition to intramolecular bonds, and the composites were crosslinked by the intermolecular disulfide bonds and π–π stacking interaction. Therefore, cations were eliminated from the oxidized composite materials, which resulted in a significant decrease of the electrostatic capacity.

3.5. Capability as battery

The charge–discharge cycle characteristics of the ANS450 cell are shown in Fig. 7. Although there was slight degradation with cycling, the ANS450 cell exhibited a high capacity of approximately 500 mAh g^{-1} at 50 cycles. The coulombic efficiency was as high as approximately 100%, which was much higher than that of the Li-sulfur cell (less than 90%). When fully charged cell was stored in an open circuit for 1 day, the Li-sulfur cell lost the capacity to less than 30%, although the Li-ANS450 cell retained the capacity of 100%. From these results, it was evident that sulfur fixation in ANS450 was effective for solving dissolution problems in the Li-sulfur cell.

Usually, organic active materials are not conductive and require large amount of conductive additives. And, the densities of the organic active materials are low. Therefore volumetric capacity of the battery using organic material has to be low, even if the gravimetric capacity is high. On the other hand, the concentration of ANS450 can be increased up to 90 wt%, and the amount of conductive additives, Ketjen black, is only 5 wt%. The cell using this cathode showed quite high capacity of 0.68 Ah g^{-1}-cathode, and the average discharge voltage was 1.8 V. The density of the intact cathode was 1.5 g mL^{-1}, which is much higher than those of usual organic materials. The volumetric capacity of the Li-ANS450 cell can be calculated to 1.8 kW L^{-1}-cathode, which has the potential to realize the ultrahigh energy density battery.

4. Conclusion

An electric charge storage device with high capacity was proposed based on a "battery with variable electrostatic capacity" idea; the electrostatic capacity, a physical quantity, is significantly changed by the redox, a chemical reaction, and the capacity of the capacitor is superimposed on the capacity of the battery.

In order to fix sulfur, a mixture of anthracene and sulfur was calcined to prepare a sulfur composite material. The composite material exhibited an extremely large capacity that was larger than the capacity estimated from the sulfur content. The electrostatic capacity of the composite material changed significantly with the redox reaction, and the basic concept of a "battery with electrostatic capacity" was validated. Close examination of the capacity generation mechanism provided evidence that the major factor of capacity increase was due to the "variable electrostatic capacity" phenomenon. The development of an electric charge storage device based on the "battery with variable electrostatic capacity" is expected in the future.

Acknowledgements

The author thanks Y. Katoh for conducting the Raman spectra measurement and simulation, N. Takahashi for XPS measurements, and T. Uyama for XRD measurements.

References

[1] E. Peled, Y. Sterberg, A. Gorenshtein, Y. Lavi, J. Electrochem. Soc. 136 (1989) 1621–1625.
[2] A. Debart, J. Bao, G. Armstrong, P.D. Bruce, J. Power Sources 174 (2007) 1177–1182.
[3] J.P. Zheng, R.Y. Liang, M. Hendrickson, E.J. Plichta, J. Electrochem. Soc. 155 (2011) A432–A437.
[4] J. Shim, K.A. Striebel, E.J. Cairns, J. Electrochem. Soc. 149 (2002) A1321–A1325.
[5] Y.V. Mikhaylik, J.R. Akridge, J. Electrochem. Soc. 151 (2004) A1969–A1976.
[6] Y. Li, H. Zhan, S. Liu, K. Huang, Y. Zhou, J. Power Sources 195 (2010) 2945–2949.
[7] R. Dominko, R. Demir-Cakan, M. Morcrette, J. Tarascon, Electrochem. Commun. 13 (2011) 117–120.
[8] L.J. Xue, J.X. Li, S.Q. Hu, M.X. Zhang, Y.H. Zhou, C.M. Zhan, Electrochem. Commun. 5 (2003) 9037–9906.
[9] K. Naoi, K. Kawase, M. Mori, M. Komiyama, J. Electrochem. Soc. 144 (1997) L173–L175.
[10] J. Li, H. Zhan, L. Zhou, S. Deng, Z. Li, Y. Zhou, Electrochem. Commun. 6 (2004) 515–519.
[11] J. Wang, J. Yang, C. Wan, K. Du, J. Xie, N. Xu, Adv. Funct. Mater. 13 (2003) 487–492.
[12] X. Yu, J. Xie, Y. Li, H. Huang, C. Lai, K. Wang, J. Power Sources 146 (2005) 335–339.
[13] C. Lai, X.P. Gao, B. Zhang, T.Y. Yan, Z. Zhou, J. Phys. Chem. C 113 (2009) 4712–4716.
[14] J.L. Wang, J. Yang, J.Y. Xie, N.X. Xu, Y. Li, Electrochem. Commun. 4 (2002) 499–502.
[15] Y.J. Choi, Y.D. Chung, C.Y. Baek, K.W. Kim, H.J. Ahn, J.H. Ahn, J. Power Sources 184 (2008) 548–552.
[16] W. Sugimoto, H. Iwata, Y. Yasunaga, Y. Murakami, Y. Takasu, Angew. Chem. Int. Ed. 42 (2003) 4092–4096.
[17] L. Kavan, J. Rathousky, M. Gratzel, V. Scklover, A. Zukal, J. Phys. Chem. B 104 (2000) 12012–12020.
[18] H. Zoh, D. Li, M. Hibino, I. Honma, Angew. Chem. Int. Ed. 44 (2005) 797–802.
[19] A.L. Briseno, Q. Miao, M-M. Ling, C. Reese, H. Meng, Z. Bao, F. Wudl, J. Am. Chem. Soc. 128 (2006) 15577–15776.

[20] Gaussian 03, Revision D.02, Gaussian, Inc., Wallingford, CT, 2004.
[21] X.L. Wen, Z.L. Liu, J.M. Lu, Y.C. Liu, J. Chem. Soc. Faraday Trans. 88 (1992) 3323–3326.
[22] Z.J. Liu, L.B. Kong, Y.H. Zhou, C.M. Zhan, J. Power Sources 161 (2006) 1302–1306.
[23] Y. Yamakita, J. Kimura, K. Ohno, J. Chem. Phys. 126 (2007) 064904.
[24] D. Aurbach, E. Pollak, R. Elazari, G. Salitra, C.S. Kelley, J. Affinito, J. Electrochem. Soc. 156 (2009) A694–A702.
[25] L.J. Xue, J.X. Li, S.Q. Hu, M.X. Zhang, Y.H. Zhou, C.M. Zhan, Electrochem. Commun. 5 (2003) 903–906.
[26] J. Chmiola, G. Yushin, Y. Gogotsi, C. Portet, P. Simon, P.L. Taberna, Science 313 (2006) 1760–1763.